Hyperfine Interactions (2020) 241:41
https://doi.org/10.1007/s10751-020-01713-3

Collinear laser spectroscopy of stable palladium isotopes at the IGISOL facility

Sarina Geldhof[1] · Paul Campbell[2] · Bradley Cheal[3] · Ruben de Groote[1] · Wouter Gins[1] · Iain Moore[1]

Published online: 10 March 2020

Abstract
Collinear laser spectroscopy on stable palladium isotopes was performed at the IGISOL facility in Jyväskylä in preparation for an experiment on its neutron-rich isotopes. Five transitions from different initial atomic states were tested, with the goal of finding the most spectroscopically efficient. The observed intensities afforded a comparison with atomic-level population predictions based on charge-exchange calculations. For some transitions hyperfine parameters of ^{105}Pd were measured, which were found to be in good agreement with literature values. A King plot analysis was performed using the measured isotope shifts and known charge radii from literature to determine the atomic field and mass shift factors.

Keywords Collinear laser spectroscopy · Palladium · IGISOL

1 Introduction

An experimental campaign to fill in the gap in optical spectroscopy data of radioactive isotopes in the region from $Z = 43$ to $Z = 47$ was started at the IGISOL facility at the Accelerator Laboratory in Jyväskylä. There are pertinent outstanding questions on the nuclear structure of neutron-rich nuclei in this region, with possible (rapid) changes in deformation and the presence of shape coexistence. These refractory elements can be produced at the IGISOL facility thanks to the chemical insensitivity of the production method. Having recently completed successful measurements on several neutron-rich silver isotopes, the next element of choice is palladium. Knowledge about the ground-state properties is needed

This article is part of the Topical Collection on *Proceedings of PLATAN 2019, 1st International Conference, Merger of the Poznan Meeting on Lasers and Trapping Devices in Atomic Nuclei Research and the International Conference on Laser Probing, Mainz, Germany 19-24 May 2019*
Edited by Krassimira Marinova, Michael Block, Klaus D.A. Wendt and Magdalena Kowalska

✉ Sarina Geldhof
sarina.m.geldhof@jyu.fi

[1] Department of Physics, University of Jyväskylä, PB 35 (YFL), 40014 Jyväskylä, Finland

[2] School of Physics and Astronomy, University of Manchester, Manchester M13 9PL, UK

[3] Department of Physics, University of Liverpool, Liverpool L69 7ZE, UK

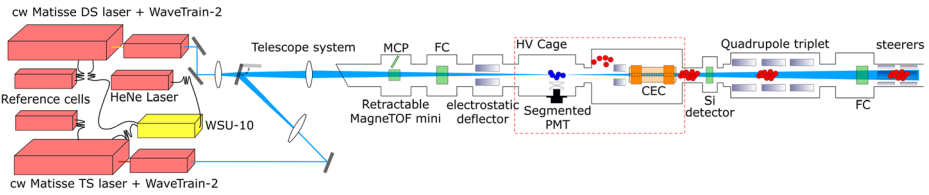

Fig. 1 Schematic view of the light collection region and laser systems of the collinear beamline at IGISOL. The ion bunches (red) enter the beamline from the right side. CEC = Charge-Exchange Cell, PMT = Photo-Multiplier Tube, MCP = Micro-Channel Plate detector, FC = Faraday Cup

to clarify the shape evolution and spin assignments in the Pd isotopic chain, as conflicting interpretations have arisen from several gamma- and beta-decay spectroscopy experiments [1–3].

In preparation for an experiment on radioactive neutron-rich isotopes, extensive offline testing was performed on all stable Pd isotopes, which is presented here. Several transitions suitable for collinear laser spectroscopy were tested in order to select the most efficient choice for online investigations. This also allowed the determination of the atomic field and mass shift factors, which are needed to extract the changes in mean-square charge radii from the isotope shifts.

2 Experimental setup

At the IGISOL facility, radioactive ion beams are produced using the ion-guide method with thin foil targets. Various offline sources are available to provide stable ion beams, such as a spark discharge source which was used in this work [4]. After production, beams are mass separated using a dipole magnet, with a typical mass resolving power of about 400, and injected into the radiofrequency quadrupole (RFQ) cooler-buncher. Ions are extracted from the cooler-buncher at an energy of 800 eV, and after passing through two 90-degree quadrupole benders are subsequently accelerated to 30 keV upon injection into the collinear beamline [5].

A schematic overview of this recently upgraded [6] beamline is shown in Fig. 1. Electrostatic deflectors guide the ions into the charge-exchange cell (CEC) and the light collection region (LCR). A quadrupole triplet is used to focus the beam in front of the Photo-Multiplier Tube (PMT). Ion and laser beams are overlapped in a counter-propagating geometry by tuning both through a removable 0.9 mm aperture. The beamline furthermore has two Faraday cups and a silicon detector which are used to optimize the transport efficiency of stable and radioactive ions, respectively. An off-axis Micro-Channel Plate (MCP) detector and a MagneTOF mini-detector mounted on a linear actuator are installed after the CEC and LCR, which are used for both beam tuning and monitoring the neutralization efficiency.

A new laser system has been installed recently to replace the Spectra Physics 380 dye laser. The new system consists of two Sirah Matisse 2 continuous wave (cw) lasers, one dye DS and one Ti:sapphire TS, both with a WaveTrain 2 frequency doubling unit. They are pumped by a 20W Spectra Physics Millenia eV laser. Both lasers have an external reference cavity to ensure short-term stability. To ensure long-term wavelength stability, these reference cavities can in turn be locked to a HighFinesse WSU-10 wavemeter using a built-in software plug-in or to a frequency-stabilized HeNe laser using a transfer cavity [7]. The (frequency-doubled) laser light required for the atomic transitions studied in this work is

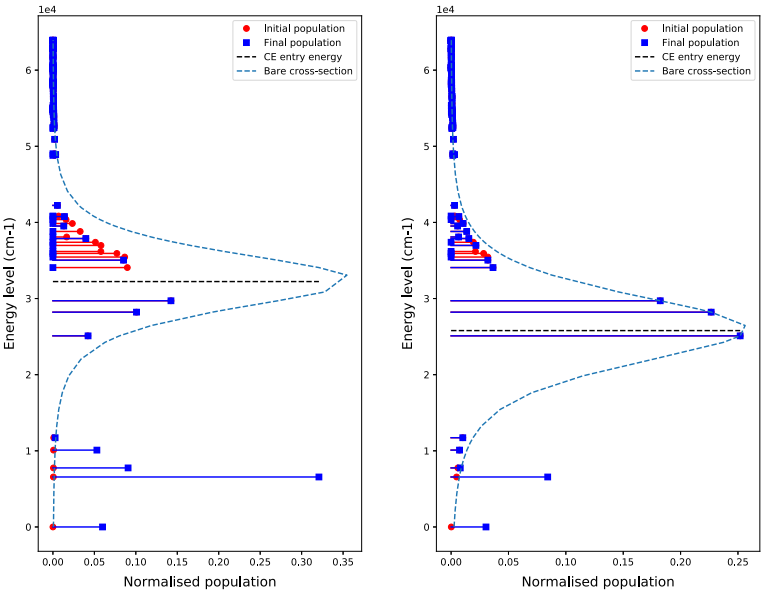

(a) K neutralizer (b) Na neutralizer

Fig. 2 Charge-exchange calculations predicting final level populations, using either (**a**) potassium or (**b**) sodium as the neutralizing vapour [8]

focused into a 1 mm spot in front of the PMT using a telescope system. Background rates due to scattered laser light are typically 100 Hz per 100 μW of laser light.

3 Results

As any strong transitions in the Pd^+ ion are inaccessible to standard continuous-wave laser systems due to the very short wavelengths, spectroscopy must be performed on the neutral atom. To this end, neutralization by passage of the ion beam through a charge-exchange cell filled with an alkali vapour is utilized. This creates a population distribution among the atomic ground state and several metastable states. From these states, five different transitions were tested which were chosen based on several considerations: the level populations predicted by charge-exchange calculations, the expected transition strength, the atomic spins involved, and the available wavelength range of the laser system. The predicted level populations were calculated with the code described in [8] for a 30 keV beam with either potassium or sodium as the neutralizing vapour. The results can be seen in Fig. 2. The most suitable transitions found in literature are from the ground state and low-lying metastable states, and thus potassium was chosen as the neutralizer as it results in significantly higher final populations for these states of interest. A neutralization efficiency of 30% was measured for Pd^+ ions via the ratio of the total detected beam on the MagneTOF mini detector to that when a deflection voltage is applied to the electrostatic deflector, indicated in Fig. 1.

An overview of the tested transitions with their electronic configurations can be seen in Fig. 3. For the 363.6-, 357.2- and 361.1-nm transitions, spectra on all six stable isotopes, ^{102,104,105,106,108,110}Pd, could be collected. Measurements using the 369.1-nm

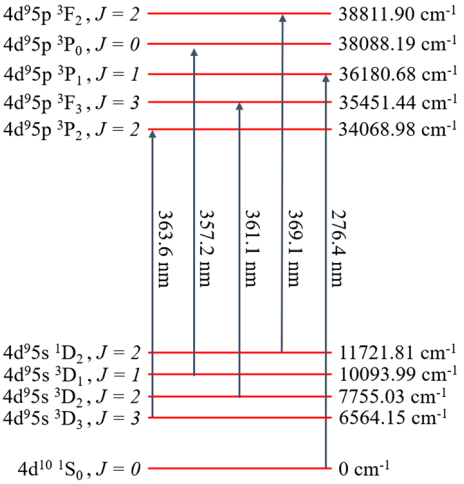

Fig. 3 Overview of studied transitions. Wavelengths are in vacuum [9]

Table 1 Measured hyperfine parameters of ^{105}Pd compared to literature. Errors on measured values are statistical errors arising from the fitting procedure

	A (MHz)		B (MHz)	
Level	This work	Literature	This work	Literature
$4d^9 5p\ ^3P_1$	−126.2(6)	−126.9(6)[a]	6(2)	2.0(9)[a]
$4d^9 5s\ ^3D_3$	−391.5(4)	−391.178(1)[b]	−650(5)	−652.906(15)[b]
$4d^9 5p\ ^3P_2$	−82.2(5)	−81(2)[c]	−302(4)	−312(7)[c]
$4d^9 5s\ ^3D_2$	64.2(4)	66.359(1)[b]	−406(4)	−398.192(10)[b]
$4d^9 5p\ ^3F_3$	−115.3(3)	−112(3)[c]	−497(4)	−536(33)[c]

[a]ref. [13] [b] ref. [14] [c] ref. [11]

transition were not pursued in detail for ^{105}Pd, which exhibits a hyperfine structure with 13 resonances, since spectra obtained on the even-A isotopes showed comparatively low efficiencies for this line. The 276.4-nm transition studied separately proved to be too low in efficiency. Only spectra for ^{105,108}Pd were obtained due to technical difficulties during this period. The low efficiency is due to a combination of a low population of the ground state and a lower quantum efficiency of the PMT at this wavelength.

All spectra were fitted using the SATLAS package [10]. For ^{105}Pd, the intensity ratios of the hyperfine components were fixed using the Racah coefficients. The hyperfine parameters obtained from the fits for ^{105}Pd on three transitions are compared to literature values in Table 1. The corresponding spectra with fits can be seen in Fig. 4. Even though a clear spectrum was obtained for the 357.2-nm transition, two of the three resonances were fully unresolved which made it impossible to reliably determine the hyperfine parameters of the lower state, so they were fixed to literature values from [11]. All measured parameters are in good agreement with previous values from literature. From the fitted centroids the isotope shifts relative to $A = 108$ have been calculated and can be found in Table 2. The included systematic error arises from the uncertainty in the determination of the cooler and acceleration voltages and was evaluated using the procedure described in [12].

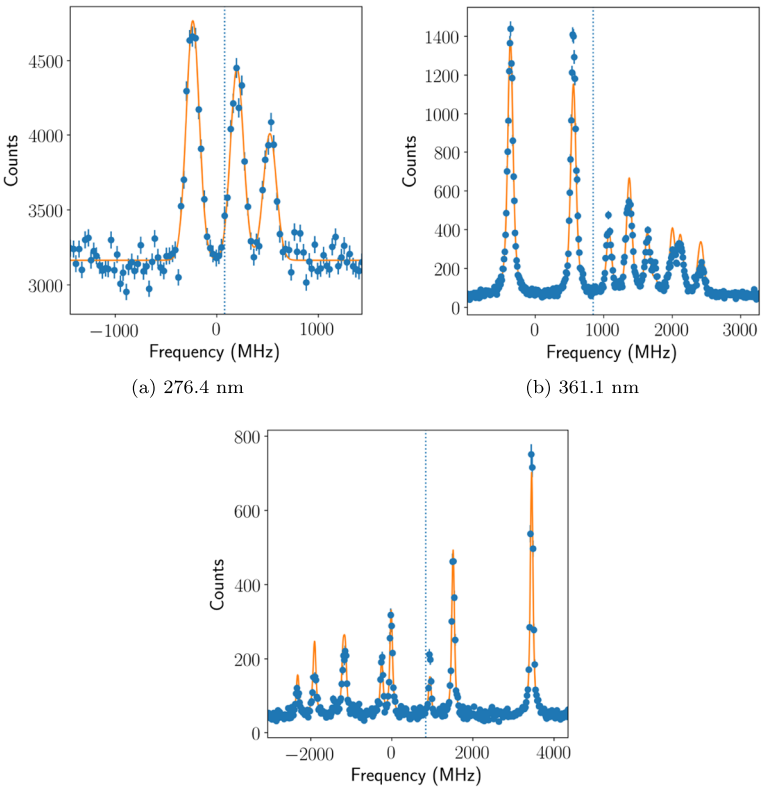

(a) 276.4 nm

(b) 361.1 nm

(c) 363.6 nm

Fig. 4 Spectra of ^{105}Pd with hyperfine fits for all transitions where hyperfine parameters could reliably be determined. Dotted lines denote the center of gravity relative to ^{108}Pd. Fitted parameters can be found in Table 1

Table 2 Measured isotope shifts. Statistical uncertainties are denoted by parentheses and systematic uncertainties due to the conversion from scanning voltages into frequencies are given in square brackets

	$\delta\nu^{108,A}$ (MHz)				
Isotope	363.6	361.1	357.2	369.1	276.4
102	1446.9(6)[190]	1413.6(14)[190]	1446(4)[20]	1337(4)[19]	/
104	954.3(5)[130]	948.4(11)[130]	958(3)[13]	889(4)[13]	/
105	836.9(7)[100]	844.7(9)[100]	842(2)[10]	/	77(3)[13]
106	492.9(5)[60]	486.2(11)[60]	490(2)[7]	464(3)[6]	/
108	0.0	0.0	0.0	0.0	0.0
110	−434.6(6)[60]	−429.4(15)[60]	−443(5)[7]	−401(3)[6]	/

In order to compare the measured peak intensities with the predicted level populations, the particle current and laser power were recorded for each scan. ^{102}Pd, the isotope with lowest abundance (1.02%), was chosen to avoid saturating the RFQ. The scaled intensities

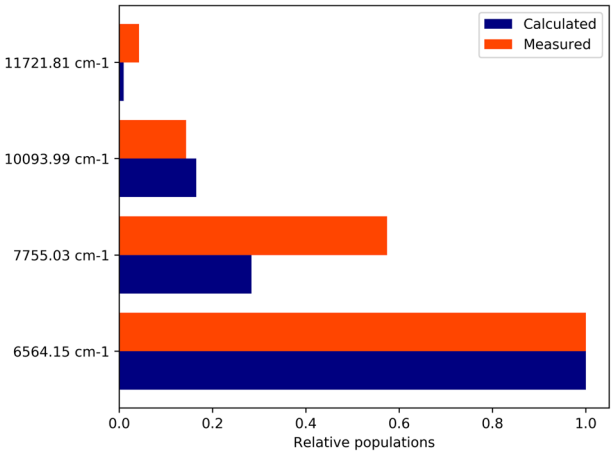

Fig. 5 Measured relative populations determined from ^{102}Pd peak intensities compared to predictions [8]

relative to the strongest level can be seen in Fig. 5. The overall order in population distribution is as expected from calculations, but the measurements suggest the 7755.03 cm^{-1} and 11721.81 cm^{-1} levels are about a factor of two more populated, or the other two levels a factor of two less. This is most likely due to decay from unknown higher-lying levels which are not included in the calculations.

The level populations are also reflected in the spectroscopic efficiencies achieved for each transition. In this work, the efficiencies are defined according to the number of photons emitted per ion detected at the end of the collinear beamline. For the 363.6-nm transition, $\sim 1/7000$ photons per ion was reached, while for the 361.1-nm transition it was $\sim 1/11000$. All other transitions had less than $1/90000$ photons/ion, making them unfeasible for experiments on neutron-rich isotopes where the number of ions at the end of the beamline is expected to vary from 2000−15000 pps for $^{112-118}$Pd, based on a combination of known fission yield cross sections, as well as scaled mass-separated yields from previously measured Ag isotopes at the IGISOL facility [15].

4 King plot analysis

The optical isotope shift between nuclei with atomic masses A and A', $\delta\nu^{A',A}$, is related to the change in mean-squared charge radii by

$$\begin{aligned}\delta\nu^{A',A} &= \nu^{A} - \nu^{A'} \\ &= \left(\frac{1}{m_{A'}} - \frac{1}{m_A}\right) M + F\delta\langle r^2\rangle^{A',A}.\end{aligned} \tag{1}$$

M and F are the transition-dependent atomic mass and field shift factors, which must be determined either theoretically or empirically via the King plot technique [16]. The King plot uses either changes in charge radii obtained from non-optical methods or known atomic

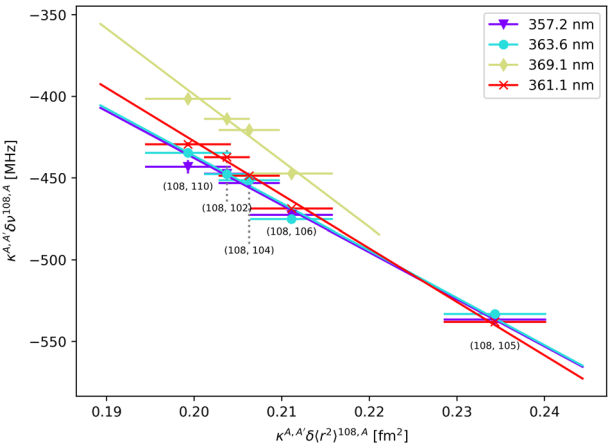

Fig. 6 King plots for all studied transitions. Modified changes in mean-square charge radii are calculated using charge radii obtained from muonic X-rays [17]

Table 3 Atomic field and mass shift factors determined using the King plot technique

Transition (nm)	Field shift (GHz/fm^2)	Mass shift (GHz amu)
363.6	−2.9(6)	845(669)
361.1	−3.3(6)	1346(773)
357.2	−2.9(6)	814(685)
369.1	−4(2)	2444(2782)

factor information from another transition to determine the atomic factors for the transition in question. Multiplying (1) with a modification factor κ,

$$\kappa^{A,A'} = \frac{m_A m_{A'}}{m_A - m_{A'}} \times \frac{m_{A_{ref}} - m_{A'_{ref}}}{m_{A_{ref}} m_{A'_{ref}}} \tag{2}$$

removes the dependence on nuclear masses and includes a standard reference pair $A_{ref} = 110$ and $A'_{ref} = 108$ for presentation. The modified isotope shifts are then written as

$$\kappa^{A,A'}\delta\nu_i^{A',A} = \frac{m_{110} - m_{108}}{m_{110} m_{108}} \times M_i + F_i \kappa^{A,A'}\delta\langle r^2\rangle^{A',A} \tag{3}$$

where i specifies the transition. The modified isotope shifts can be plotted against the modified changes in mean-squared charge radii and should yield a straight line, where the gradient contains the field shift factor and the intercept yields the mass shift factor.

In the case of palladium, the charge radii for all stable isotopes are known from muonic X-ray experiments [17]. The King plots for all transitions can be seen in Fig. 6, and the resulting field and mass shift factors in Table 3. As the field shift factor is related to the electron density at the nucleus, it is expected to be negative for transitions involving the promotion of an s-electron orbital to a p-electron orbital, as is the case for all transitions studied here. Due to the similar configurations involved, the field and mass shift factors are similar in magnitude for all transitions.

5 Summary and outlook

Offline testing on stable Pd isotopes has been performed in preparation for an experiment on neutron-rich isotopes produced in proton-induced fission of uranium. Five transitions, each with a different initial atomic state, were tested to determine the optimal approach in terms of spectroscopic efficiency and sensitivity to nuclear structure, and in order to calibrate the atomic factors. It was shown that charge-exchange calculations based on [8] provide a good starting point to choose transitions, but do not reproduce the observed populations exactly. In the end, the 363.6-nm transition from the 6564.15 cm^{-1} level showed to be the most efficient and thus the optimal choice to perform optical spectroscopy in the upcoming experiment. The atomic factors for this transition are the field shift $F = -2.9(6)$ GHz/fm^2 and mass shift $M = 845(669)$ GHz amu. These factors will allow the extraction of the unknown changes in mean-square charge radii of the neutron-rich isotopes from their isotope shifts.

Acknowledgements Open access funding provided by University of Jyväskylä (JYU). This work has received funding from the European Unions Horizon 2020 research and innovation program under Grants Agreement No. 654002 (ENSAR2). We gratefully acknowledge W. Nörtershäuser for the use of the charge-exchange cell.

References

1. Kurpeta, J., Urban, W., Płochocki, A., Rissanen, J., Elomaa, V.V., Eronen, T., Hakala, J., Jokinen, A., Kankainen, A., Karvonen, P., Moore, I.D., Penttilä, H., Rahaman, S., Saastamoinen, A., Sonoda, T., Szerypo, J., Weber, C., Äystö, J.: Excited states in ^{115}Pd populated in the β^- decay of ^{115}Rh. Phys. Rev. C **82**(027), 306 (2010)
2. Houry, M., Lucas, R., Porquet, M.G., Theisen, C., Girod, M., Aiche, M., Aleonard, M.M., Astier, A., Barreau, G., Becker, F., Chemin, J.F., Deloncle, I., Doan, T.P., Durell, J.L., Hauschild, K., Korten, W., Le Coz, Y., Leddy, M.J., Perries, S., Redon, N., Roach, A.A., Scheurer, J.N., Smith, A.G., Varley, B.J.: Structure of neutron rich palladium isotopes produced in heavy ion induced fission. Eur. Phys. J. A **6**(1), 43–48 (1999)
3. Zhang, X.Q., Hamilton, J.H., Ramayya, A.V., Zhu, S.J., Hwang, J.K., Beyer, C.J., Kormicki, J., Jones, E.F., Gore, P.M., Babu, B.R.S., Ginter, T.N., Aryaeinejad, R., Butler-Moore, K., Cole, J.D., Drigert, M.W., Jewell, J.K., Reber, E.L., Gilat, J., Rasmussen, J.O., Daniel, A.V., Oganessian, Y.T., Ter-Akopian, G.M., Ma, W.C., Varmette, P.G., Bernstein, L.A., Lougheed, R.W., Moody, K.J., Stoyer, M.A.: Identification of high spin states in neutron-rich ^{113,115,117}Pd nuclei. Phys. Rev. C **61**(014), 305 (1999)
4. Vilén, M., Canete, L., Cheal, B., Giatzoglou, A., de Groote, R.P., de Roubin, A., Eronen, T., Geldhof, S., Jokinen, A., Kankainen, A., Moore, I.D., Nesterenko, D.A., Penttilä, H., Pohjalainen, I., Reponen, M., Rinta-Antila, S.: A new off-line ion source facility at IGISOL. Nucl. Instrum. Methods Phys. Res. B **463**, 382–383 (2020)
5. Vormawah, L.J., Vilén, M., Beerwerth, R., Campbell, P., Cheal, B., Dicker, A., Eronen, T., Fritzsche, S., Geldhof, S., Jokinen, A., Kelly, S., Moore, I.D., Reponen, M., Rinta-Antila, S., Stock, S.O., Voss, A.: Isotope shifts from collinear laser spectroscopy of doubly charged yttrium isotopes. Phys. Rev. A **97**(042), 504 (2018)
6. de Groote, R.P., de Roubin, A., Campbell, P., Cheal, B., Devlin, C.S., Eronen, T., Geldhof, S., Moore, I.D., Reponen, M., Rinta-Antila, S., Schuh, M.: Upgrades to the collinear laser spectroscopy experiment at the IGISOL. Nucl. Instrum. Methods Phys. Res. B **463**, 437–440 (2020)

7. Verlinde, M., Dockx, K., Geldhof, S., König, K., Studer, D., Cocolios, T.E., de Groote, R.P., Ferrer, R., Kieck, T., Moore, I.D., Nörtershäuser, W., Raeder, S., Van den Bergh, P., Van Duppen, P., Wendt, K.: On the performance of wavelength meters - Part 1: Consequences for medium- to high-resolution laser spectroscopy. Submitted (2019)
8. Vernon, A.R., Billowes, J., Binnersley, C.L., Bissell, M.L., Cocolios, T.E., Farooq-Smith, G.J., Flanagan, K.T., Ruiz, R.F.G., Gins, W., de Groote, R.P., Koszorús, Á., Lynch, K.M., Neyens, G., Ricketts, C.M., Wendt, K.D.A., Wilkins, S.G., Yang, X.F.: Simulation of the relative atomic populations of elements $1 \leq Z \leq 89$ following charge exchange tested with collinear resonance ionization spectroscopy of indium. Spectrochim. Acta B **153**, 61–83 (2019)
9. Engleman, R., Litzén, U., Lundberg, H., Wyart, J.F.: The Pd I spectrum, term system, isotope shift and hyperfine structure – revised and extended analysis based on FTS emission spectroscopy. Phys. Scr. **57**(3), 345–364 (1998)
10. Gins, W., de Groote, R.P., Bissell, M.L., Buitrago, C.G., Ferrer, R., Lynch, K.M., Neyens, G., Sels, S.: Analysis of counting data: Development of the SATLAS Python package. Comput. Phys. Commun. **222**, 286–294 (2018)
11. Kümmel, E., Baumann, M., Kischkel, C.S.: Hyperfine structure and isotope shift in the $4d^9$ 5s configuration of Pd I. Z. Phys. D **25**(2), 161–165 (1993)
12. Voss, A., Sonnenschein, V., Campbell, P., Cheal, B., Kron, T., Moore, I.D., Pohjalainen, I., Raeder, S., Trautmann, N., Wendt, K.: High-resolution laser spectroscopy of long-lived plutonium isotopes. Phys. Rev. A **95**(032), 506 (2017)
13. van Duijn, E.J., Witte, S., Zinkstok, R., Hogervorst, W.: Hyperfine structure and isotope shift measurements on $4d^{10}\ ^1S0 \rightarrow 4d^9$ 5p $J = 1$ transitions in Pd I using deep-UV cw laser spectroscopy. Eur. Phys. J. D **19**(1), 25–29 (2002)
14. Channappa, K.H., Pendlebury, J.M.: Hyperfine structure measurements in some low-lying multiplets of ^{47}Ti, ^{49}Ti, ^{59}Co and ^{105}Pd. Proc. Phys. Soc. **86**(5), 1145–1146 (1965)
15. Geldhof, S. et al.: Collinear laser spectroscopy of radioactive Pd isotopes. Proposal to the JYFL PAC (2019)
16. King, W.H.: Isotope Shifts in Atomic Spectra. Plenum, New York (1984)
17. Fricke, G., Heilig, K.: Nuclear Charge Radii. Landolt-Börnstein/Springer, Berlin (2004)